Macromolecules

Article

Cite This: Macromolecules 2019, 52, 1757−1771

pubs.acs.org/Macromolecules

Determining the Dilution Exponent for Entangled 1,4-Polybutadienes Using Blends of Near-Monodisperse Star with Unentangled, Low Molecular Weight Linear Polymers

Ryan Hall,[†] Beom-Goo Kang,[%,¶] Sanghoon Lee,[‖] Taihyun Chang,[‖] David C. Venerus,[⊥,○,□] Nikos Hadjichristidis,[*,#] Jimmy Mays,[%] and Ronald G. Larson[*,†,‡]

[†]Department of Macromolecular Science & Engineering and [‡]Department of Chemical Engineering, University of Michigan, Ann Arbor, Michigan 48109, United States

[‖]Department of Chemistry and Division of Advanced Materials Science, Pohang University of Science and Technology (POSTECH), Pohang 37673, Korea

[⊥]Department of Chemical and Materials Engineering, New Jersey Institute of Technology, Newark, New Jersey 07102, United States

[#]Polymer Synthesis Laboratory, Physical Science and Engineering Division, King Abdullah University of Science and Technology, Thuwal 23955, Saudi Arabia

[%]Department of Chemistry, University of Tennessee, Knoxville, Tennessee 37996, United States

[○]Department of Chemical and Biological Engineering, and Center for Molecular Study of Condensed Soft Matter, Illinois Institute of Technology, Chicago, Illinois 60616, United States

Supporting Information

ABSTRACT: We determine experimentally the "dilution exponent" α for entangled polymers from the scaling of terminal crossover frequency with entanglement density from the linear rheology of three 1,4-polybutadiene star polymers that are blended with low-molecular-weight, unentangled linear 1,4-polybutadiene at various star volume fractions, ϕ_s. Assuming that the rheology of monodisperse stars depends solely on the plateau modulus $G_N(\phi_s) \propto \phi_s^{1+\alpha}$, the number of entanglements per chain $M_e(\phi_s) \propto \phi_s^{-\alpha}$, and the tube-segment frictional Rouse time $\tau_e(\phi_s) \propto \phi_s^{-2\alpha}$, we show that only an $\alpha = 1$ scaling superposes the $M_e(\phi_s)$ dependence of the terminal crossover frequency $\omega_{x,t}$ of the blends with those of pure stars, not $\alpha = 4/3$. This is the first determination of α for star polymers that does not rely on any particular tube model implementation. We also show that a generalized tube model, the "Hierarchical model", using the "Das" parameter set with $\alpha = 1$ reasonably predicts the rheological data of the melts and blends featured in this paper.

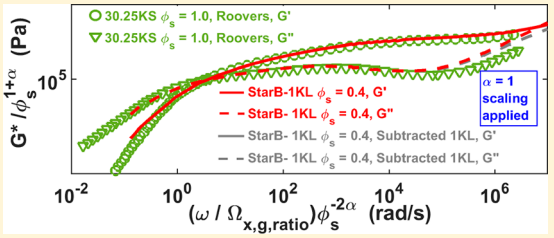

I. INTRODUCTION

The 1978−1979 publications by Doi and Edwards, "Dynamics of Concentrated Polymer Systems", laid the groundwork for the "tube theory", which, with some modifications, is still commonly used to predict the viscoelastic relaxation of polymer melts. As described in that series of papers,[1−4] polymer melt relaxation is described by a representative chain (the "probe chain") escaping the entanglements with neighboring chains. These entanglements are accounted for by a mean-field "tube" confining the probe chain. A variety of mechanisms have been identified to describe the relaxation of the probe chain out of its confining tube, in particular reptation, contour length fluctuations (CLF), and constraint release (CR), by dynamic tube dilation (DTD) and by constraint release Rouse (CR-Rouse) motion. This paper focuses on dynamic tube dilation, specifically on determining the value of the so-called "dilution exponent", α. Details regarding the other relaxation mechanisms can be found elsewhere.[5−15]

DTD describes the widening of the diameter of the tube confining the probe chain as the time-dependent entanglement constraints defining this tube at some initial time disappear by motion of surrounding chains. The DTD concept was originally applied to near monodisperse linear polymers by Marrucci[16] and then to near-monodisperse star polymers by Ball and McLeish.[17] It was later incorporated into a theory for blends of near-monodisperse stars with near-monodisperse linear polymers (both species entangled) by Milner and McLeish[18] and then used as a crucial element in general theories for polydisperse mixtures of linear and branched chains by Larson and co-workers,[19−21] by Das et al.,[22] and by van Ruymbeke and co-workers.[23] As applied to linear bidisperse and linear polydisperse polymers, DTD occurs in response to the relaxation of lower molecular weight chains,

Received: August 24, 2018
Revised: January 17, 2019
Published: February 11, 2019

DOI: 10.1021/acs.macromol.8b01828
Macromolecules 2019, 52, 1757−1771

allowing the tube containing the unrelaxed long chains to gradually explore a larger diameter tube composed of longer-lived constraints imposed by the higher molecular weight chains.[10,24−26] DTD has also been used to describe the relaxation of branched polymers, including star polymers, as described by Ball and McLeish.[17] Monodisperse star polymers are unable to undergo reptation due to the extremely limited mobility of the branch point. Thus, star arms must relax by deep CLF, and this produces a very wide range of relaxation rates for highly entangled arms, with the parts of the arm closer to its free end relaxing orders of magnitude more quickly than those parts near the branch point. The fast-relaxing parts of surrounding arms move so quickly that they act as diluents for the unrelaxed portions of the test chain. Over increasing time scales, more and more of the surrounding entanglements become "diluent" for the test chain, gradually expanding the tube diameter, until the star molecule is fully relaxed.

To employ the DTD theory, the dependence of the dilution of the entanglement density on the molecular weight between entanglements $M_e(\phi_s)$ must be quantified, where ϕ_s is the fraction of the original entanglements that are still active after relaxation has rendered the rest of them diluents. Once $M_e(\phi_s)$ is specified, the plateau modulus $G_N^0(\phi_s) = \frac{4\rho RT}{5M_e(\phi_s)}\phi_s = G_{N,0}^0\phi_s^{1+\alpha}$ is determined, where $G_{N,0}^0$ is the plateau modulus prior to dilution, as is the tube diameter $a(\phi_s) = a_0 M_e^{1/2}(\phi_s)$. The scaling of $M_e(\phi_s)$ with the dilution exponent, α, has been widely debated throughout the literature. In general, it is believed to be given by a power law, $M_e(\phi_s) = M_{e,0}/\phi_s^{\alpha}$. Some sources suggest that α should be 1,[17,27] which is consistent with viewing entanglements as discrete, mutually constraining, interactions between two chains. However, others have argued that α should be 4/3 by viewing entanglement restraints as multichain interactions within an entanglement volume.[28,29] Both values of the dilution exponent α have been widely used in tube theories, with better agreement being obtained with experimental data in some cases when one takes $\alpha = 1$, whereas other cases favor $\alpha = 4/3$.

For example, by using the value $\alpha = 4/3$, the general "Hierarchical model" deployed by Park and Larson accurately matched the experimental linear rheology of single-site catalyzed high-density polyethylene[30] as well as some 1,4-polybutadiene samples: bidispersed linear blends,[31] a nearly monodisperse star, and star-linear blends.[20,32] However, the experimental data for a mixture of linear polymers with a very large difference in molecular weight, namely 20−550 kDa 1,4-polybutadiene linear blends, required $\alpha = 1$, not 4/3, to yield acceptable agreement.[31] More generally, the literature indicates that in cases of binary blends of long and short linear chains the value $\alpha = 1$ provides predictions in agreement with experiment;[31] however, if one wishes to predict the linear rheology of both nearly monodisperse linear polymers and nearly monodisperse stars for a given polymer chemistry using the same set of model parameters, one typically must use $\alpha = 4/3$.[32] The inconsistency in choice of the value of α, with different values used by different researchers and even by the same researchers at different times, has for 20 years remained one of the most irksome problems in tube theory.[17,18,22,31−37]

In recent years, progress has been made toward resolving this issue. In particular, Huang et al.[27] have found that the moduli G' and G'' of melts diluted with oligomer of the same chemistry as the melt scale with polymer concentration in a manner consistent with $\alpha = 1$. In addition, van Ruymbeke and Watanabe[38,39] found that for binary linear blends $\alpha = 1$ at early relaxation times but that the *effective* value of α shifts to $\alpha = 4/3$ at late times due to "tension re-equilibration", which enables the longer chains to escape long-lived entanglements via a combination of constraint release and contour length fluctuations. This shift from $\alpha = 1$ to an effective dilution exponent value of $\alpha = 4/3$ was investigated further by Shahid et al.,[40] who considered long linear polystyrenes diluted with polystyrene oligomers to determine the scaling of the plateau modulus and the terminal relaxation time. They determined that good fits to the G' and G'' data were provided by a version of the tube model (the time-marching algorithm, TMA) which contained both constraint release and contour length fluctuations, when using $\alpha = 1$. The apparent rubbery modulus G_δ extracted directly from the data scaled with the concentration c of long chains as c^2, in accord with the scaling expected for $\alpha = 1$ when the number Z_2 of entanglements of a long chain with other long chains exceeded around 12, but scaled as $c^{8/3}$, in accord with $\alpha = 4/3$ for $Z_2 < 12$. Because the TMA tube model predicted both regimes correctly using a fixed value of $\alpha = 1$, the apparent transition from $\alpha = 1$ to $\alpha = 4/3$ at low Z_2 could be taken to be a consequence of tension re-equilibration. A similar transition was observed in the scaling of the terminal relaxation time from that predicted using an effective dilution exponent of $\alpha = 1$ to a higher value of α at $Z_2 < 20$. The conclusion of these studies is that at least for long linear chains mixed with their unentangled oligomers, fundamentally the dilution exponent is $\alpha = 1$; but when long chains are not highly self-entangled, additional relaxations lead to changes in *apparent* scaling laws consistent with a slightly higher value of $\alpha = 4/3$. Interestingly, Shahid et al.[40] also observed that when mixed with a small-molecule solvent rather than an oligomer, an apparent value of α higher than unity is found even for highly self-entangled polymers.

At the same time, new light has been shed on the proper value of α for branched architectures. In a study described in Desai et al.,[41] the "Hierarchical" version of the tube model successfully predicted the relaxation behavior of a pure 24 kDa star (24KS) and pure 58 kDa linear (58KL) polymer using $\alpha = 4/3$ but predicted very poorly the behavior of the 24KS−58KL blends. Modifications of tube theory entailing combinations of different CR-Rouse treatments, dilution exponents ($\alpha = 4/3$ or 1), and entanglement thresholds did not yield consistently accurate predictions of these and other star/linear blends, using either the Hierarchical model or another general-purpose model, the branch-on-branch "BoB" model developed by Das et al.[22] On the other hand, it was shown by Desai et al. that the "clustered fixed slip-link model" (CFSM), developed by Schieber et al.,[42] gave very good predictions of the 24KS−58KL blends, which could be attributed to its handling of constraint release dynamics. Details of the CFSM are discussed elsewhere.[42−47] For our purposes, the important point is that since the CFSM takes an entanglement to be a binary interaction between a pair of chains, the accurate predictions by the CFSM of the pure 24KS, pure 58KL, and 24KS−58KL blends suggest that the dilution exponent, α, should be unity for star polymers, linears, and blends. However, the failure of the most advanced versions of the tube model, using $\alpha = 1$ or 4/3, to predict correctly the rheology of the blends, suggests that the tube model is not yet accurate enough to trust the fitting of its predictions to experimental data to determine unambiguously the value of α.

DOI: 10.1021/acs.macromol.8b01828
Macromolecules 2019, 52, 1757−1771

Thus, the value of α has remained controversial largely because it is typically assigned based on agreement of the tube model with experimental data. This confounds the accuracy (or lack thereof) of tube model physics with the value of the dilution exponent. This problem is particularly acute for branched polymers, where existing tube models seem to be less accurate than for linear polymers. In principle, however, the dilution exponent can be measured directly by diluting the entangled polymer with a solvent that does not alter chain configurations of the entangled polymer. This can be accomplished by using either a theta solvent or a solvent that is close enough to being a theta solvent for the polymer concentration used that the excluded volume "correlation blob" size is smaller than the "thermal blob" size.[48,49] If this is achieved, one could in principle determine α in a "model-free" way by plotting the plateau modulus $G_N^0(\phi_s)$ against the concentration ϕ_s of entangled polymer, which should yield a power law with exponent $1 + \alpha$. Such a plot has been made,[36] but the values $\alpha = 1$ or 4/3, respectively corresponding to exponents 2.0 and 2.33 for $G_N^0(\phi_s)$, are hard to distinguish with confidence in such a plot.

A property that is much more sensitive to α is the terminal time for relaxation of a star polymer. The relaxation time of a star arm is expected, and observed, to be exponentially dependent on the number of entanglements per arm, $M_a/M_e(\phi_s) \propto M_a/\phi_s^{-\alpha}$ where M_a is the arm molecular weight. Thus, if one blends a monodispersed star with an isofrictional theta-like solvent to dilute the density of entanglements, the resulting diluted star should possess nearly the same terminal time (to within a prefactor that depends weakly on molecular weight) of a lower molecular weight, nondiluted star of the same chemistry, with the same value of $M_a/M_e(\phi_s) = M_a/(M_{e,0}\phi_s^{-\alpha})$. Because the terminal relaxation time is exponentially dependent on $M_a/(M_e\phi_s^{-\alpha})$, this putative "self-similarity" or matching of terminal relaxation time will be much more sensitive to the dilution exponent α than is the modulus, which scales only as a power law $G_N^0(\phi_s) \propto \phi_s^{1+\alpha}$. However, four important caveats arise. First, one needs a theta-like solvent, in which the replacement of some of the polymer chains by the solvent does not alter the configurations of the remaining chains. The second caveat for attainment of an equality in relaxation time is that the solvent is "isofrictional" with the polymer, so that the monomeric drag coefficient acting on the polymer is not changed by replacement of polymer with solvent. This "isofrictional" criterion is hard to meet; however, there is no need to fulfill this requirement if the change in friction produced by the addition of solvent can be accounted with reasonable accuracy. The third caveat is that the prefactor of the exponential dependence of relaxation time on $M_a/(M_e\phi_s^{-\alpha})$ be properly accounted for. The fourth caveat is that the terminal relaxation time, *or its equivalent*, be properly measured at sufficiently low frequencies where rheological data can become noisy or sensitive to small contributions from high-molecular-weight tails. The second and third caveats both deal with the frictional prefactor of the exponential dependence of relaxation time on $M_a/(M_e\phi^{-\alpha})$, and so results are not as sensitive to the accuracy with which they are accounted for as they are to the value of α.

We propose here to determine the α value by performing a series of dilutions of star polymers with subentangled linear polymer of the same chemistry, where the subentangled linear polymer serves as an approximately isofrictional theta-like solvent, as described above. Because the "solvent" used here is itself 1,4-polybutadiene, with chemistry nearly identical to the entangled star polymers (although with slight differences in 1,2 content), this "solvent" should be approximately a theta solvent as well as approximately isofrictional. We qualify this remark by the word "approximately" because, although the monomers are chemically nearly identical to that of the star, the small size of the linear chain implies that it might have some osmotic swelling power with respect to the much larger star polymer, and the linear chain might have somewhat smaller monomeric friction coefficient because of a dependence of the glass transition on molecular weight, which is quite weak for well-entangled polymers but becomes more pronounced for smaller chains. As to the swelling power of the short linear chain, we remark that our blends all contain at least 20 vol % star polymer, implying that the correlation "blob" size is quite small, likely smaller than the size of the "thermal blob". Without getting into details here, we simply note that when this is the case, the high molecular weight star chain is ideal on all length scales, and the solvent is then effectively a theta solvent even if it is not perfectly so at low star polymer concentration. This is called the "concentrated" regime, to distinguish it from the "semidilute" regime in which swelling of the long polymer chain occurs over length scales between that of the thermal blob and the correlation (or excluded-volume) blob. In studies of small-molecule solvents with polystyrene,[48] Heo and Larson showed that a transition from semidilute to concentrated solutions occurred once the concentration was raised to 20% polymer or so for a good solvent (tricresyl phosphate) for polystyrene. Hence, for short 1,4-polybutadiene chains, which should have weaker swelling power for long 1,4-polybutadiene than small-molecule tricresyl phosphate has for polystyrene, we expect that long polymers at concentrations of 20% or more should have nearly ideal (i.e., nonswollen) conformations.

A more important concern is the change in monomeric friction coefficient produced by dilution of the long star chains with much shorter linear chains. To evaluate such changes in friction, it is important to gather data at high frequency for a variety of temperatures, where frictional effects are most clearly distinguished from the confounding effects of entanglement dynamics. The change in the monomeric friction, along with the known scaling of the Rouse relaxation time of an entanglement segment with M_e, namely $\tau_e(\phi_s) \propto M_e^2 \propto \phi_s^{-2\alpha}$, allows for the effect of added solvent on the fundamental time constant of the tube model, $\tau_e(\phi_s)$, to be accounted for in a model-insensitive way.

Motivated by this background, here we present linear rheology measurements of three symmetric approximately 4-armed 1,4-polybutadiene stars diluted with a 1000 Da linear 1,4-polybutadiene. These stars have arm molecular weights M_a of approximately 48, 61.5, and 70.1 kDa, hereby termed StarA, StarB, and StarC, respectively. Details of synthesis will be discussed below as well as characterization using gel permeation chromatography (GPC) and temperature gradient interaction chromatography (TGIC). The quality of these star polymers is further evaluated via rheological measurements which are compared to established trends in the literature for star 1,4-polybutadiene polymers. Each of these stars is blended with the nearly monodispersed 1 kDa linear 1,4-polybutadiene, hereby termed 1KL obtained from Polymer Source; its quality is verified via GPC and rheology. Following the preparation of the star−1KL blends, these samples are subjected to a series of small-amplitude oscillatory shear rheology tests over a range of

DOI: 10.1021/acs.macromol.8b01828
Macromolecules 2019, 52, 1757−1771

temperatures to produce viscoelastic G' and G'' master curves, which are compiled using time−temperature superposition.

To determine the value of the dilution exponent α from these curves without relying on a specific tube model, and its various assumptions, and to avoid difficulties in the accurate determination of the terminal relaxation time (i.e., the fourth caveat mentioned above), we extract the low-frequency crossover modulus, $G_{x,t}$, and frequency, $\omega_{x,t}$, from these data and plot them in properly scaled form against entanglement density $M_a/M_e(\phi_s)$ on "universal" plots for both $\alpha = 1$ and $\alpha = 4/3$. The validity of using the crossover frequency $\omega_{x,t}$, rather than the terminal relaxation time, to assess the dilution exponent rests on the dependence of all tube model (and slip-link model) predictions on only three nonuniversal parameters: a frictional time constant (such as the equilibration time τ_e), a modulus scale (such as the plateau modulus G_N^0), and the number of entanglements per chain Z. The first two of these constants set the frequency and modulus scales of the rheology and can be removed in dimensionless plots. The parameter Z determines not only the terminal relaxation time *but in principle also the shape* of the relaxation function (e.g., G' or G'' against frequency ω). Thus, both a rescaled terminal time τ_t/τ_e and a rescaled terminal crossover frequency $\omega_{x,t}\tau_e$ should be a universal function of Z for any polymer architecture (such as a monodisperse star). But this universal function will depend on the value of the dilution exponent α, and for stars diluted with a theta-like solvent, even the value of Z itself depends on α. Nevertheless, if we guess a value of α and compute the values of Z for a series of diluted stars, the dependence of $\omega_{x,t}\tau_e$ on Z should be the same for the diluted stars as for a series of undiluted stars of various molecule weights *if we have guessed the right value of* α. We carry out this exercise in what follows for both $\alpha = 1$ and $\alpha = 4/3$. The results show that the $\alpha = 1$ scaling of star−1KL data within the $\omega_{x,t}$ versus $M_a/M_e(\phi_s)$ plot are in agreement with data for pure stars, whereas the $\alpha = 4/3$ scaling fails. The data in the plot of $G_{x,t}$ versus $M_a/M_e(\phi_s)$ are not surprisingly inconclusive due to the plot's lack of sensitivity of $G_{x,t}$ to the value of α. While our procedure requires us to perform many experiments to determine the dependence of $\omega_{x,t}\tau_e$ on Z for a variety of star concentrations, this procedure is advantageous in greatly increasing the robustness of our conclusion since it is insensitive to random errors in characterization or rheology of individual samples and averages out such errors. Establishing the value of α without invoking model specifics is critical considering the that the dynamic dilution theory of the tube model has had difficulty in describing simultaneously both mechanical and dielectric data for star polymers, as summarized by McLeish.[50] These results suggest that we cannot rely on good agreement between tube model predictions and star polymer rheological data to determine the appropriate value of α. After establishing the correct value of α experimentally, we also predict the blend rheological data using the Hierarchical model, leading to reasonably good agreement with the experimental data sets for $\alpha = 1$.

II. MATERIALS AND EXPERIMENTAL METHODS

II.1. Materials and Preparation. The three nominally 4-arm 1,4-polybutadiene star polymers (StarA, StarB, and StarC) featured in this study were carefully synthesized and characterized via temperature gradient interaction chromatography (TGIC) and gel permeation chromatography (GPC) to ensure that they are nearly monodisperse or at least that they are entirely star polymers with nearly monodisperse arm length and no linear contaminants. Details regarding the synthesis and molecular weight characterization of these 1,4-polybutadiene samples can be found below and in the Supporting Information. As an added level of inspection, the molecular weights of the star samples were further verified by fitting rheological predictions from the Hierarchical 3.0 model with experimental data resulting from small-amplitude oscillatory shear (SAOS) rheological measurement. Because previous studies have shown that this model predicts the rheological response of pure star molecules well, the model can help confirm the accuracy of the molecular weight assignments from GPC and TGIC.

The linear 1,4-polybutadiene in this study has a molecular weight of ∼1 kDa, hereby referenced as 1KL, with "K" indicating the molecular weight in kDa and "L" the linear architecture. Because the entanglement molecular weight for 1,4-polybutadiene is $M_{e,0} = 1.62$ kDa (using the so-called "G definition"[51] of M_e), and the crossover molecular weight to the entangled regime is 2−3 times higher than this, the 1KL sample in this study is well within the unentangled regime. This linear polymer was obtained from Polymer Source, which reported the polydispersity as 1.1. Because this material acts as a diluent, its precise molecular weight (and molecular weight distribution) is unimportant as long as it is unentangled with itself and we account experimentally for this linear polymer's effect on the monomeric friction coefficient of the blend.

Blends of star and 1KL samples were prepared in accordance with the procedure detailed in Desai et al.[41] The StarA−1KL blend series contains star volume fractions ϕ_s of 1, 0.6, 0.4, 0.2, and 0. The StarB−1KL series has ϕ_s of 1, 0.5, 0.4, 0.2, and 0. And finally, the StarC−1KL series has ϕ_s of 1, 0.6, 0.5, 0.4, 0.2, and 0.

II.2. Synthesis. All three 4-arm 1,4-polybutadiene stars were synthesized via anionic polymerization, high-vacuum techniques and chlorosilane chemistry, using custom-made glass reactors equipped with break-seals for the addition of reagents and constrictions for removal of aliquots.[52] The synthetic procedure is given in Scheme 1.

Scheme 1. General Reactions for the Synthesis of 4-Arm Stars 1,4-Polybutadiene

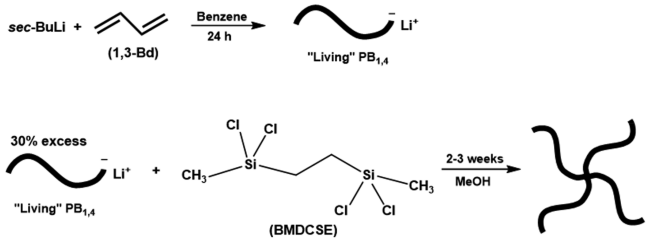

A nonpolar solvent (benzene) was used to ensure the highest 1,4 microstructure of PBds, and a linking agent (1,2-bis-(dichloromethylsilyl)ethane, BMDCSE) having two chlorines instead of four ($SiCl_4$) per silicon atom was used to ensure complete replacement of the chlorines by 1,4-polybutadiene chains.[53,54] Details of the synthesis are given in the Supporting Information.

II.3. Characterization. The 1,4-polybutadiene stars featured in this study were characterized via gel permeation chromatography (GPC) and temperature gradient interaction chromatography (TGIC). For further verification of the arm molecular weights reported by GPC and TGIC, two separate predictions from the Hierarchical 3.0 model were generated for comparison with linear viscoelastic shear rheological data of each of the pure stars. One prediction was obtained by implementing the model with the "Park" parameter set,[20] and the other prediction was generated by utilizing the "Das" parameter set.[22] The key difference between these two parameter sets (which are given later in this paper) is that the Park parameter set utilizes a dilution exponent of $\alpha = 4/3$, while for the Das set, $\alpha = 1$. As mentioned previously in this paper, α is a parameter that characterizes dynamic tube dilation, which is crucial for capturing the relaxation behavior of branched polymer architectures. Further details of the Hierarchical model and its parameter sets are given in

DOI: 10.1021/acs.macromol.8b01828
Macromolecules 2019, 52, 1757−1771

the Results and Discussion section. We simply note here that for monodisperse star polymers both the Hierarchical model and the "Bob" model are equivalent to the Milner−McLeish theory for star polymers.[33]

All three stars were intended to contain four arms, which is consistent with GPC, TGIC, and rheological characterization for StarB and StarC. However, both GPC and TGIC data for the postfractionated StarA, shown in Figure 1, indicate that it is

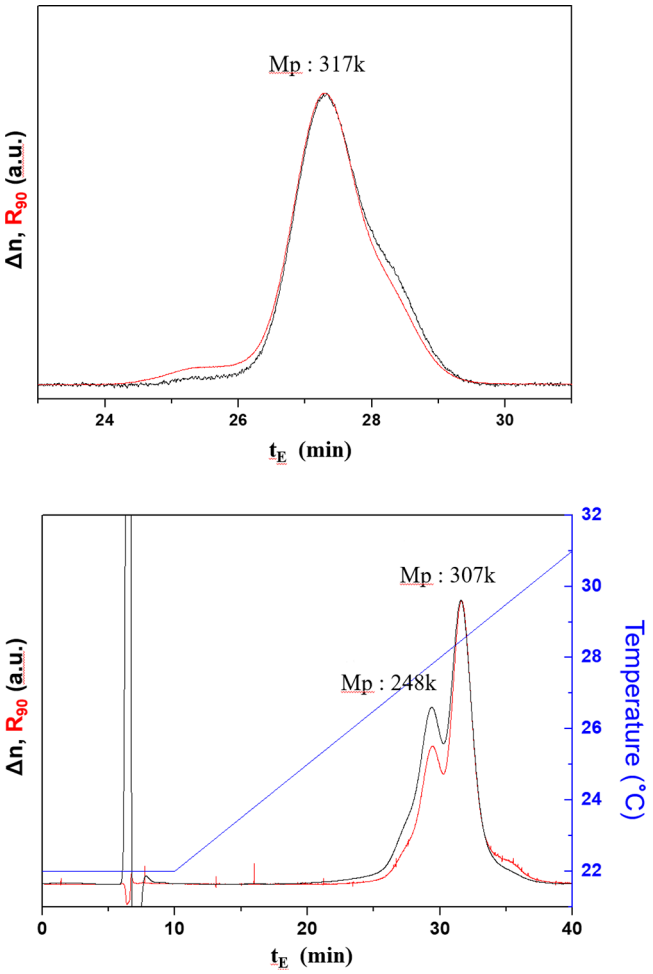

Figure 1. Elution profiles from gel permeation chromatagraphy (top) and temperature gradient interaction chromatography (bottom) for StarA. The *y*-axes are the differential refractive index (Δn), which is represented by the black line, and the light scattering intensity determined at a 90° angle (R_{90}), represented by the red line.

polydisperse in the number of arms per molecule. The TGIC chromatogram shows two distinct peaks, which likely correspond to stars possessing 4−8 arms per molecule. The associated GPC plot in Figure 1, which displays a broad peak indicating polydispersity, is consistent with the TGIC chromatogram. Because of the ambiguity in the number of branches in StarA, we report in Table 1 the molecular weight determinations of the linear precursor arms of StarA, which are 47 kDa from GPC and 49.1 kDa from TGIC, and nearly monodisperse. We note that it is only the molecular weight of the arm that matters, not the number of arms, since both experiments and theory show that the rheology is independent of the number of star branches and of polydispersity in the number of branches, as long as there are no linear contaminants or star species with more than 10 arms. Of this we can be confident, based not only on the TGIC and GPC chromatograms but also on the rheological data themselves, as we shall soon see.

Table 1. Star Arm Molecular Weights Derived from GPC and TGIC Star Peak for StarB and StarC and from the Arm Peak for StarA as Well as through Fits by the Hierarchical Model by Using Both Das and Park Parameters

	GPC (kDa per arm)	TGIC (kDa per arm)	Hierarchical park (kDa per arm)	Hierarchical das (kDa per arm)
StarA	47	49.1	50.4	48
StarB	65[a]	70[a]	65.5	61.5
StarC	71.3[a]	72.5[a]	76	70.1

[a]The MW was calculated by dividing the star MW by 4.

Shown in Figures 2 and 3 are the GPC and TGIC results for StarB and StarC, respectively. For StarB, Figure 2 shows that the linear

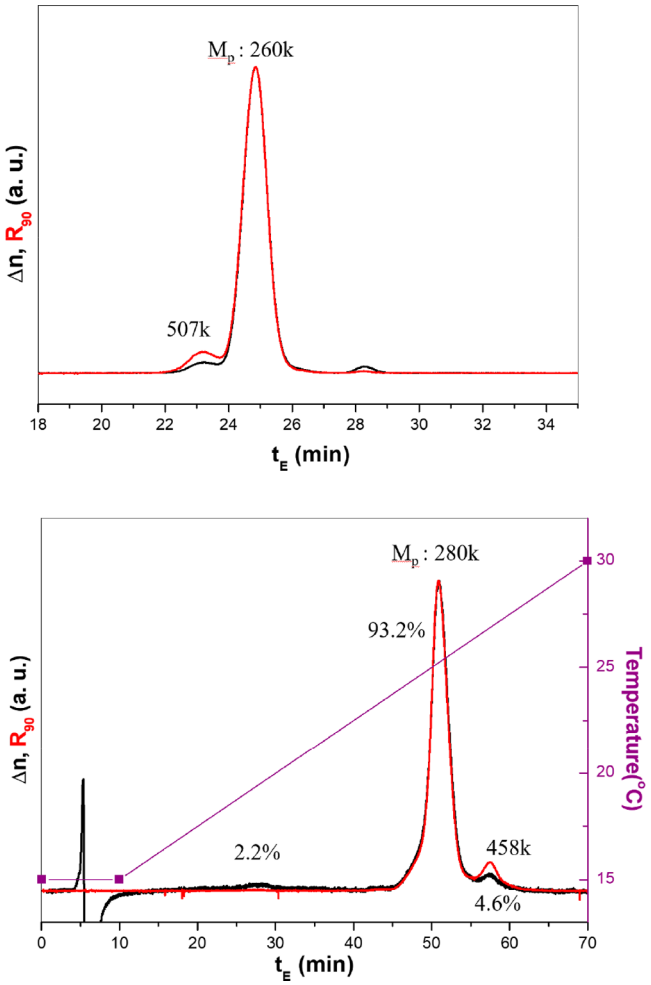

Figure 2. Same as Figure 1, but for StarB.

precursor is almost entirely gone after fractionation. Prior to fractionation, TGIC and GPC reported for the linear precursor a molecular weight of 68 kDa. Dividing this into the molecular weight of the main peak (260K for GPC and 280K for TGIC) gives very close to four for the number of arms. No direct data on the arm molecular weight for StarC are available. But according to Figure 3, when we divide the molecular weight of the main peak (285K for GPC and 290K for TGIC), assuming four arms per molecule, we obtain arm molecular weights of 71.3K for GPC and 72.5K for TGIC for StarC. Note the presence of substantial side peaks in the TGIC trace for StarA in Figure 1 and their absence for StarB and StarC in Figures 2 and 3, respectively. Both StarB and StarC show a narrow molecular weight distribution (M_w/M_n = 1.01−1.03) and very little

DOI: 10.1021/acs.macromol.8b01828
Macromolecules 2019, 52, 1757−1771

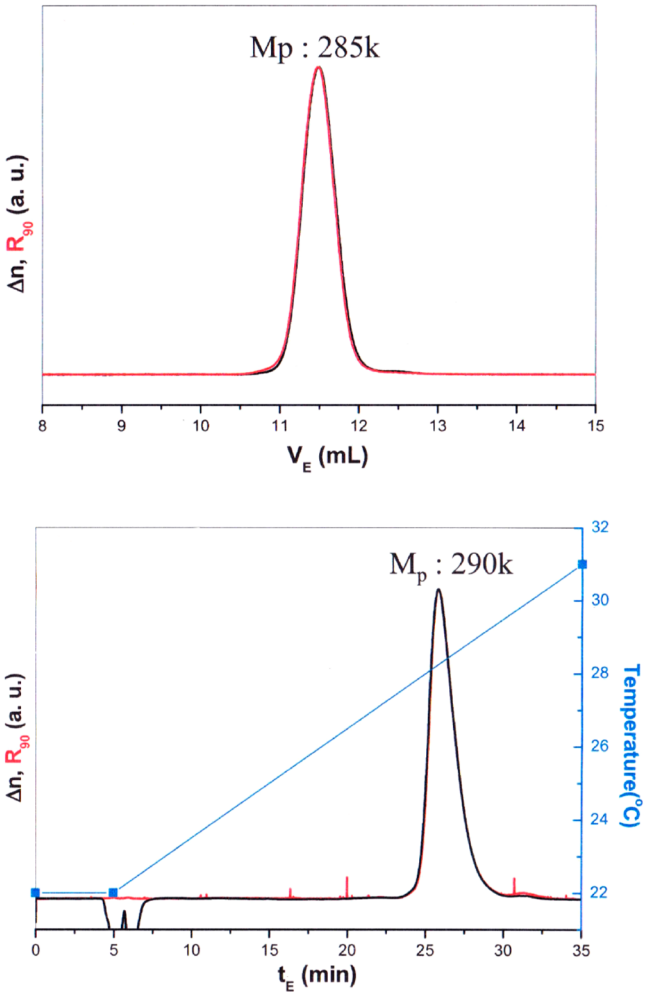

Figure 3. Same as Figure 1, but for StarC.

presence of side peaks, indicating a nearly pure four-arm star in each case.

In addition to these characterizations, we can estimate the arm molecular weights from application of the tube model, which has been found to fit well the rheology of pure star for a variety of 1,4-polybutadiene stars of various molecular weights.[19−21,32,41] Thus, we can also assign the arm molecular weights of all three stars according to predictions from the Hierarchical model, using both Das and Park parameters. This gives us four ways to determine arm molecular weight: GPC, TGIC, and tube model fittings using both Das and Park parameters. As will be seen, results are very similar for all four methods of determining molecular weight.

Table 1 gives the star arm molecular weights reported by GPC and TGIC of our three stars, along with the arm molecular weights obtained from fitting Hierarchical model predictions, using both Park and Das parameters, to the rheology of these melts. The Hierarchical model fit for StarB will be shown below, while those for StarA and StarC are given in the Supporting Information. For StarA, the GPC and TGIC results are taken from the molecular weight of the precursor arm, while for StarB and StarC, the molecular weight of the star was divided by four to obtain the arm molecular weight. Table 1 indicates differences of up to 9 kDa among the arm molecular weights derived from GPC, TGIC, and tube model predictions. These uncertainties in molecular weight have in previous work generally limited the confidence with which such data can be used to test model predictions, especially for stars, whose rheology is extremely sensitive to arm molecular weight. Thus, to mitigate these uncertainties, here we will test our conclusions using all four of the molecular weights given in Table 1 for each polymer and will not rely on fits of the tube model predictions to rheological data to get a "best" value of α. Instead, we will use the low-frequency crossover frequency of G' and G'' and its scaling with molecular weight and dilution with low molecular weight linear polymer, for multiple star polymers, to derive a robust conclusion regarding the exponent α that is not sensitive to the uncertainty in molecular weight of the arm.

II.4. Rheology. Small-amplitude oscillatory shear (SAOS) rheological measurements were performed on ARES-LS and RMS 800 rheometers to obtain linear viscoelastic G' and G'' data. Tests were conducted using 25 and 8 mm parallel plates. Strain-controlled frequency sweeps, ranging from 0.1 to 100 rad/s, were performed at various temperatures from 50 to −105 °C. The TA Orchestrator software was implemented for analyzing the rheological data and generating master curves. A horizontal shift factor, a_T, at each temperature was obtained via the Williams−Landel−Ferry equation. A vertical shift, b_T, was implemented to account for changes in temperature only; the density of the 1,4-polybutadiene was taken as constant. The resulting master curves all have a reference temperature of 25 °C. The shift factors for the StarB−1KL blend series can been seen in Figure 5. The shift factors for the StarA−1KL and StarC−1KL blend series, along with "van Gurp−Palmen" plots that reveal the quality of the shifting, can be viewed in the Supporting Information. These plots indicate very good superposition at all temperatures except the lowest (below −85 °C).

III. RESULTS AND DISCUSSION

We report in Figure 4 the WLF horizontal shift factors obtained through time−temperature superposition of G' and G'' linear rheology data for the 1,4-polybutadiene pure StarB, StarC, and 1KL (symbols). (We note that StarA is not included because this sample was depleted prior to rheological testing at temperatures below 25 °C.) As discussed in Park et al.,[55] we can estimate roughly the 1,2-vinyl content of our pure stars through comparison of horizontal shift factors with those of other 1,4-polybutadienes, with varying 1,2-vinyl content, found throughout the literature. The larger the 1,2 content, the higher is the low-temperature shift factor. The vinyl content of these literature 1,4-polybutadienes is shown in parentheses within the legend, along with their respective backbone architectures. In this plot, we observe the shift factors of the pure StarB superpose closely with the shift factors of a 11% 1,2-vinyl content linear reported by Palade et al.[56] On the basis

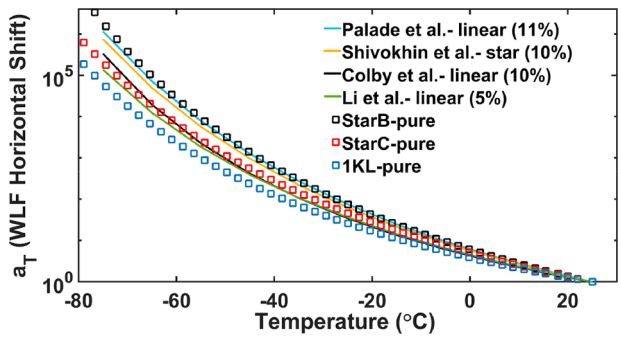

Figure 4. Shift factors plotted with respect to temperature given by the WLF equation with C_1 and C_2 time−temperature superposition constants reported for each of the materials. The pure stars of 1,4-polybutadiene chemistry explored in this study (symbols) are compared with other 1,4-polybutadiene polymers (lines), of varying 1,2-vinyl content, found throughout the literature.[55−59] The backbone architecture (star or linear) is noted in the legend along with their respective 1,2-vinyl content shown in parentheses. The reference temperature for this and all subsequent figures following (except for Figure 7) is 25 °C.

DOI: 10.1021/acs.macromol.8b01828
Macromolecules 2019, 52, 1757−1771

of this observation, we estimate that the 1,2-vinyl content for the pure StarB is approximately 11−12%. On the other hand, we observe the shift factors of pure StarC at low temperature are close to those reported by Colby et al.,[57] which report 1,2-vinyl contents of around 10%, and not far from those of Li et al.,[58] who report 5% 1,2-vinyl content. Therefore, the 1,2-vinyl content of our StarC polymer is between around 5% and 10%. Lastly, we observe a notable difference in shift factors between the pure 1KL and that of the other 1,4-polybutadienes featured in Figure 4, as can be expected. The pure 1KL is subentangled; thus, its monomeric friction coefficient is lower than the well-entangled melts, which ultimately contributes to this observed difference in shift factors. Because of this difference in the monomeric friction coefficient between the pure 1KL and well-entangled melts featured in Figure 4, we are unable to estimate the 1,2-vinyl content of the 1KL. However, having explicit knowledge of the 1,2-vinyl content of the 1KL is not necessary for this study, as can be seen in what follows.

Figure 5 plots the shift factors obtained through the time−temperature superposition of the StarB−1KL blend series.

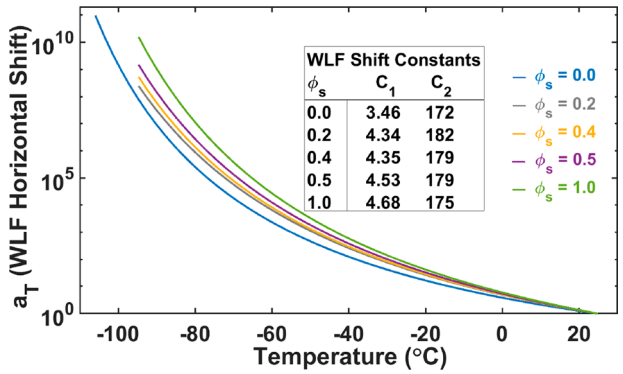

Figure 5. Shift factors obtained from time−temperature superposition of G' and G'' for StarB−1KL blends with various star volume fractions, ϕ_s.

StarB experiences a reduction in its monomeric friction coefficient with increasing concentration of 1KL, presumably due to a reduction in the glass transition temperature, because of the increasing number of chain ends. The effect of this becomes large at low temperatures. For instance, the horizontal shift factor for the pure StarB at −95 °C is about 2 orders of magnitude larger than the horizontal shift factor for the pure 1KL at the same temperature.

Appearing in Figure 6 are the linear viscoelastic G' and G'' curves of the StarB−1KL blend series produced by time−temperature superposition. The presence of the 1 kDa linear chain significantly shortens the terminal relaxation time of StarB. Although the full terminal relaxation behavior for the pure StarB is not experimentally captured due to the low frequencies required to do so, the plot does capture the terminal G'/G'' frequency crossover (ω_x), whose inverse (ω_x^{-1}) can be taken as an estimate of the terminal relaxation time. The value of ω_x increases with increasing 1KL content, with ω_x for ϕ_s = 0.5 exceeding ω_x for the pure StarB by 3 orders of magnitude. Also evident in Figure 6 is the effect of the 1KL diluent on the plateau modulus (G_N^0) of the StarB. Because it is unentangled, the short linear 1 kDa chain reduces the number of effective entanglements of the star arm by increasing the molecular weight between entanglements (M_e)

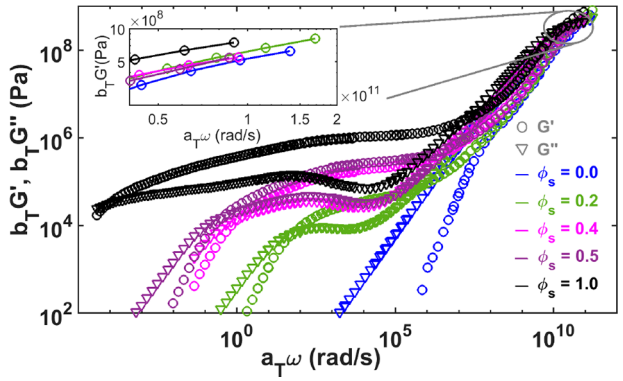

Figure 6. G' and G'' for the StarB−1KL blend series, obtained via time−temperature superposition. The insert expands the high frequency region for G'.

following the equation $G_N^0 = \frac{4\phi_s\rho RT}{5M_e}$, where we are here using the so-called "G" definition for M_e.[50] Note also that the pure StarB passes from the transition region to the rubbery plateau region at a higher frequency than do the StarB−1KL blends due to the larger tube diameter of the blends and consequent larger range of frequencies over which local Rouse modes dominate the response.

The inset within Figure 6 features G' in the transition region to the glassy plateau, which indicates a shift to higher frequencies of the pure 1KL polymer and of the blends relative to the pure StarB as a result of the shift in the glass transition temperature alluded to above. The shifting along the frequency axis of the G' curves is roughly monotonic with star content; however, the G' curves of all blends, from ϕ_s = 0.2 to ϕ_s = 0.5, are almost coincident, although they are well separated from the curve for the pure star and, to a lesser extent, from that for the pure short linear polymer. One possible reason for the lack of a greater spread among the curves for these blends with composition in the range ϕ_s = 0.2 to ϕ_s = 0.5 might be accuracy limitations of the rheometer, which arises from two possible sources. First, the moduli values of these 1,4-polybutadiene samples near the glassy plateau are closer to the elastic modulus for the rheological tooling, which is made of steel (the elastic modulus for steel is roughly 200 GPa); thus, the tooling may experience some compliance if the strain posed on the samples is too large, which results in a reduction in G^* as determined by the rheometer (although we minimized this by using 8 mm diameter plates). Second, the response of the 1,4-polybutadiene samples becomes increasingly elastic near the glassy plateau, and there is a chance that the rheological tooling may experience wall slip with the samples. Note that testing samples near their glassy plateau requires the use of strains as low as 0.16% to help reduce wall slip. Errors from these possible sources seem to be modest, however, since there were no obvious anomalies in the frequency dependence of the data, other than the near overlap of data for the blends. Also, as described in the Supporting Information, the other two sets of star/linear blends show almost identical high-frequency behavior. Thus, it seems unlikely that there is any unsystematic error in our data, as might be caused by sporadic slip phenomena.

We also note here an analogous study of a 61-armed 1,4-polybutadiene star with an arm molecular weight of 47.5 kDa, hereby termed 47.5KS ("K" represents "kDa" and "S" represents star architecture), blended with a 1 kDa linear by

DOI: 10.1021/acs.macromol.8b01828
Macromolecules 2019, 52, 1757−1771

Miros et al.[59] Featured in Figure 7 are some G' curves from their blend series, showing that blending of the 1 kDa linear

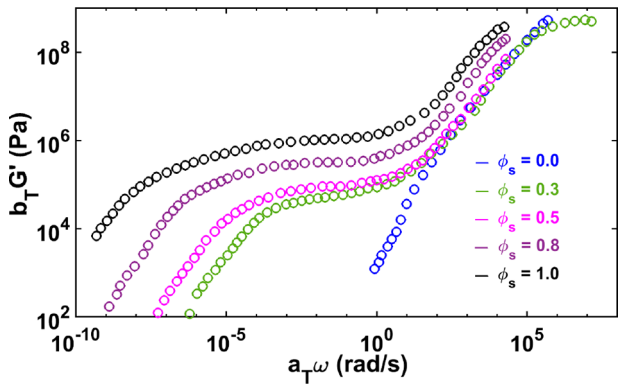

Figure 7. Experimental G' curves for the 47.5KS−1KL blend series at a reference temperature of −83 °C. Reproduced with permission from ref 60. Copyright 2003 Society of Rheology.

polymer with the pure 47.5KS caused significant shifts of the G' curve from ϕ_s = 1.0 to ϕ_s = 0.8 to ϕ_s = 0.5, which indicates a notable change of the free volume available at the chain ends. However, increased 1KL concentration beyond ϕ_s = 0.5 did not produce significant shifts in the G' behavior. Our results are somewhat analogous to the results from Miros et al., since we also see little shift between ϕ_s = 0.5 and ϕ_s = 0.2; however, we do see a small shift when the star volume fraction drops from 0.2 to 0, which Miros et al.[60] did not see.

From these observations, we can judge that the high-frequency data for our blends are likely quite accurate, despite some suspicions due to the near identity of the high-frequency data over the composition range ϕ_s = 0.2 to ϕ_s = 0.5. Because the curves shift along the frequency axis by a total of a factor of 3 over the entire composition range from ϕ_s = 0 to ϕ_s = 1, we can, in all probability, assess that any error is significantly less than a factor of 2 shift along the frequency axis. While the behavior of the polymer in this glassy region is not the focus of this study, we will use the high-frequency crossover of G' and G'' to correct for changes in monomeric friction coefficient in our analysis of the composition dependence of the terminal frequency crossover below. Hence, we take note here of the magnitude of possible error in the high-frequency rheology and show below that a possible error of a factor of 2 would not change the conclusions of our work.

We now seek to use the data of Figure 6 and the analogous data for the two other blend series to determine the dilution exponent independently of details specific to a particular tube model. To do so, we focus on the scaling of the terminal regime with entanglement density, tuned by a combination of arm molecular weight and star volume fraction. To avoid invoking modeling details, we use only the scaling of the three tube parameters with star concentration, namely the plateau modulus (G_N^0), the entanglement molecular weight (M_e), and the equilibration time (τ_e). As a metric of the horizontal and vertical shifting of the terminal regime, we take the low-frequency crossover modulus $G_{x,t}$ and frequency $\omega_{x,t}$ at which the G' and G'' curves intersect in onset of the terminal regime. While it is expected that the inverse of the terminal relaxation time $1/\tau_1$ differs from $\omega_{x,t}$ to a degree that depends on the molecular weight and concentration of polymer, tube theories generally imply that the product $\omega_{x,t}\tau_1$ depends only on the number of entanglements per chain Z, whether this is reduced by reducing molecular weight or concentration of the polymer. Hence, our method of scaling described below should in principle apply equally well to either $\omega_{x,t}$ or to τ_1. Note that this conclusions rests on the assumption that the only three material-dependent parameters controlling the linear rheology are G_N^0, τ_e, and Z. The possibility that this might not be the case is discussed at the end of the paper. As noted previously, since the 1KL is subentangled and shares the same chemistry as the pure StarB, the 1KL is here treated as a theta solvent, which means that we can simply scale the tube model parameters, using the dilution exponent, according to eqs 1−3:

$$G_N^0(\phi_s) = G_{N,0}^0 \phi_s^{1+\alpha} \tag{1}$$

$$M_e(\phi_s) = \frac{4\phi_s \rho RT}{5G_N^0(\phi_s)} \propto \phi_s^{-\alpha} \tag{2}$$

$$\tau_e(\phi_s) = \frac{M_e(\phi_s)^2 \zeta(\phi_s) b^2}{M_0{}^2 3\pi^2 kT} \propto \frac{\zeta(\phi_s)}{\zeta_0}\phi_s^{-2\alpha} \propto [\omega_{x,g,0}/\omega_{x,g}(\phi_s)]\phi_s^{-2\alpha} \propto \phi_s^{-2\alpha}/\Omega_{x,g,\text{ratio}} \tag{3}$$

The variables in eq 2 are the entanglement molecular weight (M_e), polymer density (ρ), gas constant (R), temperature (T), and the plateau modulus (G_N^0), which is given in eq 1. Once eq 2 has been solved, the resulting entanglement molecular weight can be used in eq 3 to solve for the equilibration time (τ_e), which also involves the monomeric friction coefficient (ζ), statistical segment length (b), monomer molecular weight (M_0), Boltzmann constant (k), and temperature (T). After rescaling the equilibration time of the melt to account for the star volume fraction using the factor $\phi_s^{-2\alpha}$, an additional correction must be applied to account for changes in the monomeric friction coefficient due to the presence of the 1KL. As can be seen in Figure 6, the presence of the 1 kDa linear chain horizontally shifts the experimental G' of the blends to higher frequencies due to the reduced monomeric friction coefficient. Therefore, in addition to rescaling the melt equilibration time by the factor $\phi_s^{-2\alpha}$, it must also be multiplied by the ratio of monomeric friction coefficients of the solution to the melt $\frac{\zeta(\phi_s)}{\zeta_0}$, as shown in eq 3. Because the high-frequency crossover frequency should be proportional to the inverse of the monomeric friction coefficient, to obtain the equilibration time of the blend from that of the pure star, we must divide the latter by the glassy frequency crossover ratio, $\Omega_{x,g,\text{ratio}} \equiv \omega_{x,g}(\phi_s)/\omega_{x,g,0}$ which is the ratio of the glassy crossover frequency of the respective star−1KL blend to that of the pure star. This scaling allows us to horizontally shift experimental data to correct for changes in monomeric friction coefficient because of dilution with the 1KL linear polymer.

We note that there is an alternative to using the high-frequency crossover frequency to determine the shift in the rheological curves due to the effect of dilution with 1KL linear polymer. We could instead use the curve of shift factor versus temperature near the reference temperature to determine an "isofrictional temperature" and plot data shifted to this temperature for each blend. That is we can use WLF plots of the shift factor versus temperature for each blend and find the shift in temperature "ΔT_g" needed for each blend to map the blend shift factor plot onto that of the pure star. This, in principle, allows us to shift data for each blend to a

DOI: 10.1021/acs.macromol.8b01828
Macromolecules 2019, 52, 1757−1771

temperature that is theoretically the same distance from the glass transition temperature as for the pure star. This should correct for the change in T_g produced by the blending with 1KL linear polymer, for each blend, without needing the high-frequency data to determine the shift. This "isofrictional" temperature shifting is especially useful for high-T_g polymers, such as polystyrene, for which a single master curve, extending into the glassy region, is not possible. Such a method was used, for example, by Wagner.[61] We carry out a similar analysis here, presented in the Supporting Information, and find again that superposition of terminal frequency $\omega_{x,t}$ is achieved for $\alpha = 1$ and not for $\alpha = 4/3$. The similarity of the result obtained using an isofrictional temperature analysis to that obtained by shifting using the high-frequency crossover is not surprising since 1,4-polybutadiene obeys time−temperature superposition much better across a wide range of frequencies into the glassy region than does polystyrene, for example.

Figure 8 plots the terminal crossover modulus ($G_{x,t}$) versus the effective number of entanglements per star arm, scaled in

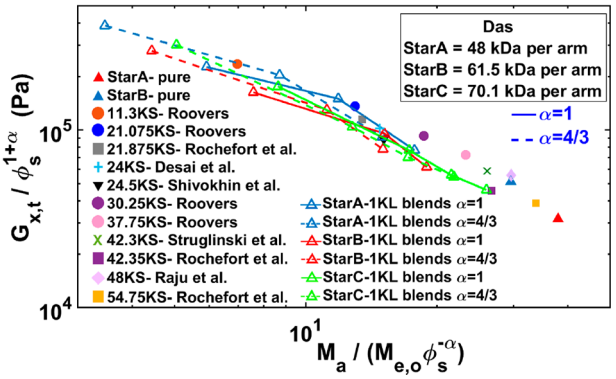

Figure 8. Terminal crossover modulus plotted against the effective number of entanglements per star arm, with both axes scaled appropriately for the concentration of star ϕ_s, taken from the experimental data for the star−1KL blends featured in this paper (open symbols), as well as from pure 1,4-polybutadiene stars ($\phi_s = 1$) from our work and from the literature (closed symbols).[35,41,59,62−64] For each polymer, the arm molecular weight is given by the numerical value in the legend. The pure-star arm molecular weights of the new stars in our study (StarA, StarB, and StarC) are given by fits to predictions made with the Hierarchical model implemented with Das parameters. For the blends, two versions of each data point are given; the points obtained using $\alpha = 1$ are connected by solid lines, while those for $\alpha = 4/3$ are connected by dashed lines. The number of entanglements is obtained by dividing the arm molecular weight by the entanglement molecular weight, which for pure stars is taken as $M_{e,0} = 1.62$ kDa.

accordance with eq 1 to account for the dilution effects of the 1KL polymer. The arm molecular weights of the new stars featured in this study are taken from fitting the Hierarchical model implemented using Das parameters, as mentioned earlier and given in Table 1. Use of the other molecular weights in Table 1 yields similar plots. Along the x-axis, the effective number of entanglements is obtained by scaling $M_{e,0}$, which is the entanglement molecular weight of the pure star, with $\phi_s^{-\alpha}$ and taking $M_{e,0} = 1.62$ kDa. The scaling was done for both $\alpha = 1$ and $\alpha = 4/3$, with solid lines in Figure 8 linking the data scaled using $\alpha = 1$ and dashed lines for those scaled using $\alpha = 4/3$. There is of course no need to apply any scaling for data sets for the pure stars (given by solid symbols) from our work and from the literature.[35,41,59,62−64] From Figure 8, the data for the blends (open symbols) favor either of the α values, $\alpha = 1$ and $\alpha = 4/3$, approximately equally. Therefore, we conclude that the dependence of $G_{x,t}$ on M_e does not provide enough sensitivity to the small difference in α values to determine which value is preferred. Although not shown, plots generated from star arm molecular weights reported from GPC, TGIC, and the Hierarchical model Park parameters prediction, as given in Table 1, lead to the same conclusion.

The ambiguity in determining α from the composition dependence of $G_{x,t}$ motivates examining the dependence of terminal crossover frequency, $\omega_{x,t}$, on the effective number of entanglements per star arm, which is featured in Figure 9. This

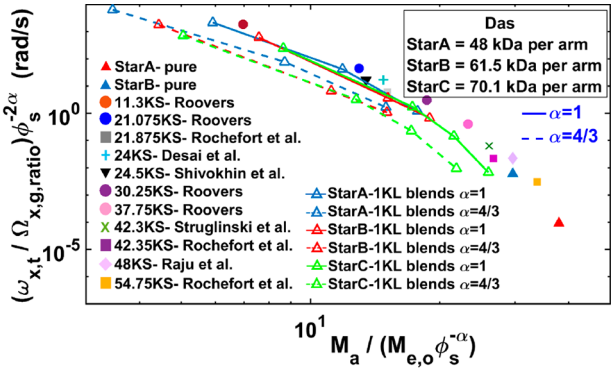

Figure 9. Rescaled terminal crossover frequency vs the effective number entanglements of experimental star-linear data using the molecular weights determined by fitting of the Hierarchical model with Das parameters to the pure melt data for StarA, StarB, and StarC. In addition to rescaling to account for the concentration of star, the change in friction due to the short linear chain is scaled out using the ratio $\Omega_{x,g,ratio}$ of the crossover frequencies near the glassy plateau of the blend to that of the pure star, as discussed in the text. Other details are the same as in Figure 8.

plot is generated using star arm molecular weights defined by fits of the Hierarchical model using Das parameters. Figures 10−12 are similar plots developed based on the other

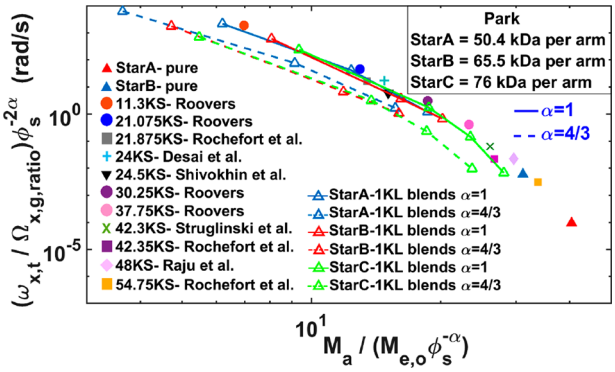

Figure 10. Same as in Figure 9, except that the molecular weight assignments for StarA, StarB, and StarC were obtained from fits of the pure melt data to the Hierarchical model with Park parameters.

estimates of molecular weight given in Table 1. (Readers who prefer to rely on experimental characterization of molecular weight should feel free to ignore results in Figures 9 and 10, which are based on fits to the tube model.) Also, the effective number of entanglements is scaled in the same way as in Figure 8, where $M_{e,0}$ is taken as 1.62 kDa. To properly scale

DOI: 10.1021/acs.macromol.8b01828
Macromolecules 2019, 52, 1757−1771

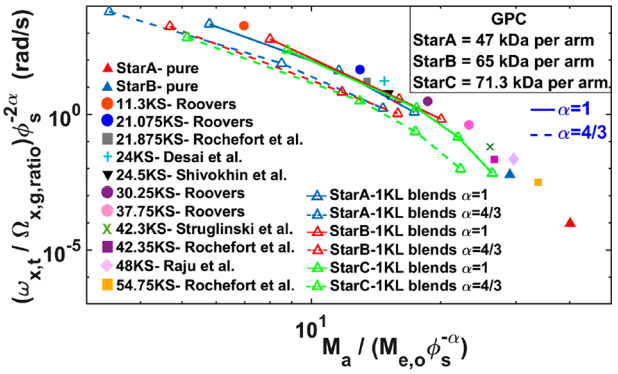

Figure 11. Same as in Figure 9, except that the molecular weight assignments for StarA, StarB, and StarC were obtained from GPC analysis.

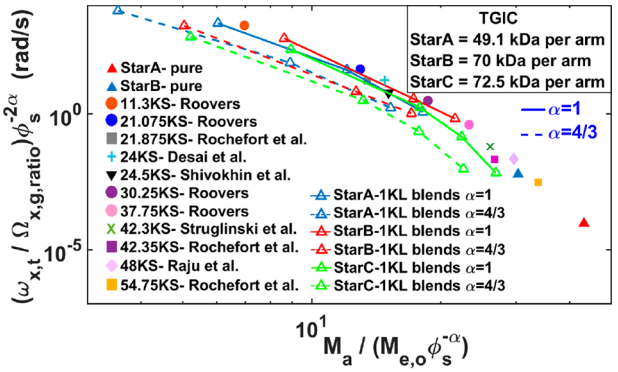

Figure 12. Same as in Figure 9, except that the molecular weight assignments for StarA, StarB, and StarC were obtained from TGIC analysis.

the vertical axis, $\omega_{x,t}$ must be adjusted to account for the reduction in the monomeric coefficient caused by the presence of the 1KL in the star−1KL blends. As shown in Figure 6, the presence of the 1KL causes the glassy plateau crossover for the StarB−1KL blends to shift to roughly 3-fold higher frequencies with respect to the pure star. Therefore, in Figure 9, the terminal crossover frequency of each blend is divided by the ratio of the crossover frequency near the glassy plateau of a given blend to that of a pure star, $\Omega_{x,g,\mathrm{ratio}}$, as discussed earlier (see eq 3). In addition, as described above, $\omega_{x,t}$ needs to be corrected for changes in τ_e due to the dilution effects of the 1KL in the star−1KL blends, again according to eq 3. With these corrections, unlike the results in Figure 8, Figure 9 displays a clear distinction (a decade difference along the y-axis) in the star−1KL blend scaling between $\alpha = 1$ vs $\alpha = 4/3$, with the blend data clearly superimposing better onto the pure star data when $\alpha = 1$ (solid lines) than when $\alpha = 4/3$ (dashed lines). We note that these results are robust. Even if we do not account for changes in the monomeric friction coefficient through the use of $\Omega_{x,g,\mathrm{ratio}}$ for the scaling of the terminal crossover frequency, the conclusion that $\alpha = 1$ coalesces the data better than does $\alpha = 4/3$ would still stand. We also note that each of the three blend series, those involving StarA, StarB, and StarC, show the same clear superiority of $\alpha = 1$ over $\alpha = 4/3$. Thus, if the blue open symbols in Figure 9, which are data from StarA, whose characterization might be questioned (as discussed above), are ignored, the conclusion that $\alpha = 1$ provides the clear best fit remains solid. We note that there is substantial scatter in the data in Figures 9−12, substantially exceeding the estimated maximum error (factor of 2) in the value of $\Omega_{x,g,\mathrm{ratio}}$. This additional scatter is likely due to random errors in characterization, some impurities in the sample, and/or errors in rheometry. However, such errors, if random, do not undermine the conclusion we draw here, since we only rely on the overall superposition of blend data on top of pure star data to establish the correct value of α. Deviations of results for individual samples are averaged out by our procedure, again showing the robustness of our method.

Thus, plotting the rescaled terminal crossover frequency against entanglement length clearly establishes $\alpha = 1$ as the only value of the dilution exponent consistent with any version of the tube model. This conclusion is independent of the particular tube model chosen, since any such model has behavior that is universal when plateau modulus and entanglement time are used to scale the modulus and time scales with the number of entanglements per chain as a sole parameter. Not only does Figure 9 establish the correct dilution exponent for the tube model (at least when applied to star polymers), but the value $\alpha = 1$ also is the only value consistent with slip-link models that treat slip-links as entanglement interactions between two chains. Thus, had our results for blends not coalesced with those for pure stars when using $\alpha = 1$, then our blend data would not be consistent with typical slip-link models.

To test the sensitivity of our conclusion to characterization errors, we replot in Figures 10−12 our star−1KL blend data from Figure 9, using arm molecular weights of the pure stars resulting from TGIC, GPC, and Hierarchical model predictions implemented with Park parameters, as given in Table 1. For Figures 9−12, we observe that $\alpha = 1$ gives clearly the superior agreement with melt data. Thus, our conclusion is independent of the uncertainties in the arm molecular weights reported by our characterization approaches. Moreover, any one of the three star blend series suffices to draw the same conclusion, and hence the ambiguities and uncertainties in our characterizations are very unlikely to undermine the conclusion that only $\alpha = 1$ can properly account for the dilution effect.

As additional evidence that $\alpha = 1$ provides the correct scaling, we compare in Figure 13 the scaled G' and G'' curves for the blend StarB−1KL $\phi_s = 0.4$, which are represented as red lines, with those for a pure 30.25KS, which are shown as

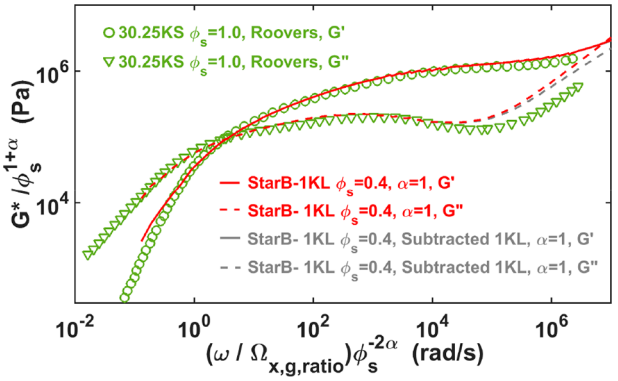

Figure 13. G' and G'' curves for the StarB−1KL $\phi_s = 0.4$ blend scaled using $\alpha = 1$ (red lines). Contributions from the 1KL are subtracted (gray lines) from the scaled StarB blend for comparison. Also featured are unscaled data for a pure 30.25KS (light blue symbols) of Roovers.[62] The y- and x-axes for the blend are scaled in accordance with eqs 1 and 3, respectively.

DOI: 10.1021/acs.macromol.8b01828
Macromolecules 2019, 52, 1757−1771

symbols. This 30.25KS, which was taken from Roovers,[62] has almost the same value of number of entanglements per star arm as in the StarB−1KL blend with ϕ_s = 0.4, if α = 1. Figure 13 shows agreement in both the terminal and plateau regions between the pure 30.25KS and the StarB−1KL blend data scaled using α = 1. Note that the high-frequency upturn in G'' occurs at lower frequency in the blend than in the pure 30.25KS because the linear polymer present in the blend (but absent in the pure star) begins to contribute to the rheology in this regime. We show some evidence of this by subtracting away the 1KL contribution to the blend, as indicated by the gray line. The 1KL subtraction yields negligible difference in the profile of the StarB blend in the terminal regime and at lower frequencies of the plateau region. However, as we approach frequencies at which Rouse modes begin to dominate the relaxation, we observe a deviation between the original G'' data for the blend and that with the 1KL data subtracted. While we cannot use the pure star to prepare an analogous plot using α = 4/3, since the entanglement molecular weight would not agree with that of the blend if α = 4/3, we will show below other plots that indicate the failure of α = 4/3 to provide agreement between Hierarchical model predictions and the linear rheological data.

We now compare our experimental results with viscoelastic predictions of the Hierarchical 3.0 model for one of the three sets of blends. These comparisons will show that while the model does not give perfect agreement with the data, the terminal behavior of the blends is generally fitted significantly better using α = 1 than using α = 4/3, consistent with the findings reported above. There are two parameter sets commonly used within the Hierarchical and other tube models for 1,4-polybutadiene melts at 25 °C: those of Park et al.[20] and of Das et al.[22] Each parameter set is composed of four key variables: the equilibration time (τ_e), the plateau modulus (G_N^0), the entanglement molecular weight (M_e), and the dilution exponent (α). For details concerning the origin of the Park and Das parameters, please consult Wang et al.[21] The Park parameter set uses α = 4/3, whereas that of Das uses α = 1. The density values for 1,4-polybutadiene needed to obtain the corresponding Park and Das entanglement molecular weights from the plateau moduli using $G_N^0 = \frac{4\rho RT}{5M_e}$ differ slightly: 894 kg/m^3 for Park parameters and 899 kg/m^3 when solving for Das parameters. The Park equilibration time requires that the value for the monomeric friction coefficient to be 5.08 × 10^{-11} kg/s, whereas for the Das parameters it is ζ = 2.94 × 10^{-11} kg/s. Note that for both Park and Das parameters the equilibration time was determined by fitting rheology data for linear or star 1,4-polybutadienes, and the friction coefficients are not available other than by backing them out from eq 3, using the fitted τ_e.

Featured in Figure 14 are the rheological data for the pure 1 kDa linear polymer along with a comparison of Hierarchical model predictions (lines) of the pure StarB sample with the experimental rheological data for this star (symbols). The legend within the figure lists the Park and Das parameters for a pure star. We observe that both the Das and Park parameters can capture the terminal relaxation of the pure star; however, the molecular weights were adjusted to obtain these fits in each case. The Park parameters require an arm molecular weight of 65.5 kDa, whereas the Das parameters require 61.5 kDa. These Das and Park molecular weights are the values given in Table 1 and are used in Figures 9 and 10. This difference in these

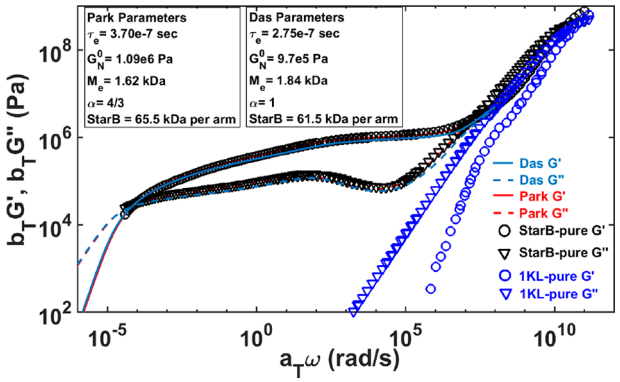

Figure 14. Hierarchical model predictions of Park (red lines) and Das (blue lines) of pure StarB data (black symbols). The inserted legend lists the Das and Park parameters of the pure star. Also plotted are the viscoelastic curves of pure 1KL data (blue symbols).

molecular weights is primarily caused by the dilution exponent used: the Park parameters uses α = 4/3, whereas the Das parameters uses α = 1. We utilize these two different molecular weights to fit the rheological data for the pure StarB to have an unbiased basis for assessing the accuracy of the predictions for each value of α when unentangled linears are blended with the pure star. We note that the fits using the Das and the Park parameters are almost equally good for the pure star and that the difference in the Das and Park molecular weights required for these fits is only 4 kDa, which is within the error of the characterization of these stars. This comparison in Figure 14 illustrates well the futility of trying to ascertain the value of α from fits of tube model predictions to one or even several different polymers: small differences in molecular weight, that are well within experimental uncertainty, can easily skew the conclusion regarding the proper value of α. Thus, the conclusion drawn from directly diluting the melt is much superior to that obtained by fitting a particular tube model to the data for pure melts. The latter depends on the accuracy of the molecular weight assignment and the accuracy of the particular tube model used, while the former only depends on scaling laws for the tube parameters and not on model details or even on the precise value of the molecular weight. Lastly, we want to mention that no Hierarchical predictions were made for the pure 1KL in Figure 14 because the Hierarchical model fails to account for the combination of Rouse and glassy modes that dominates the relaxation of such low molecular weight melts.

Featured in Figures 15−17 are predictions and data for StarB−1KL blends of star volume fractions (ϕ_s) 0.5, 0.4, and 0.2, respectively. The comparison of Hierarchical predictions with experimental data for the StarA−1KL and StarC−1KL blends can be found in the Supporting Information. These figures, including Figures 15−17 and those in the Supporting Information, show that the terminal crossover frequency for the blends is always better predicted when using the Das data set with α = 1 than when using α = 4/3. Also shown in Figures 15−17 are experimental data with the influence of 1KL subtracted out. This is done to assess the experimental data independently of the 1KL contribution to the Rouse and glassy modes. As mentioned earlier, the Hierarchical model is unable to predict the relaxation behavior of the 1KL melt or its contribution to the rheology of the star polymers because the model does not account for the combination of Rouse and glassy modes, which is a dominating feature of the 1KL. The

DOI: 10.1021/acs.macromol.8b01828
Macromolecules 2019, 52, 1757−1771

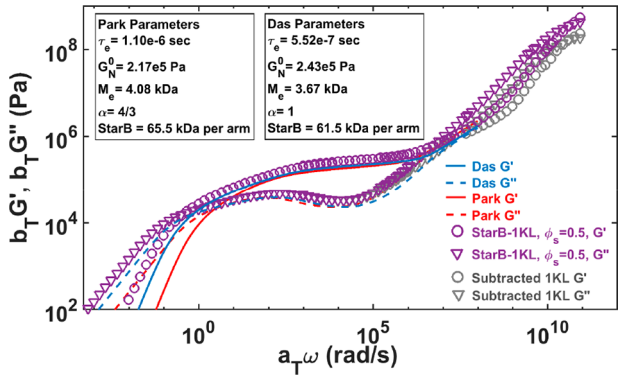

Figure 15. Scaled Hierarchical model predictions using Park (red lines) and Das (blue lines) parameters compared to data (symbols) for 50% StarB with 1KL. Predictions use scaled parameters given in the legends, with plateau modulus $G_N^0(\phi)$, entanglement molecular weight $M_e(\phi)$, and equilibration time $\tau_e(\phi)$ obtained from eqs 1−3, with α = 4/3 for Park parameters and α = 1 for Das parameters, and the parameters for the pure melt given in the legend to Figure 14. Also featured are experimental results with the influence of the 1KL linear subtracted from the original experimental data, as described in the text (gray symbols).

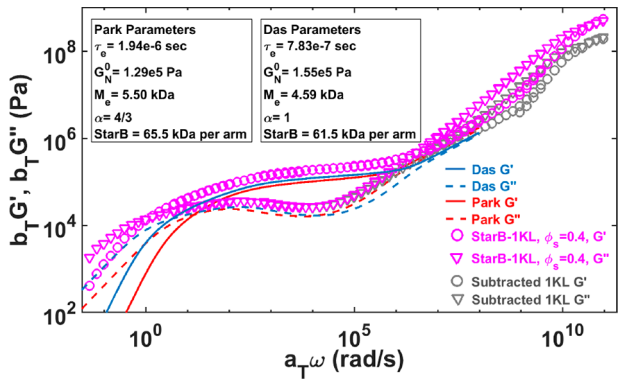

Figure 16. Same as in Figure 15, except for the 40% S−60% L blend.

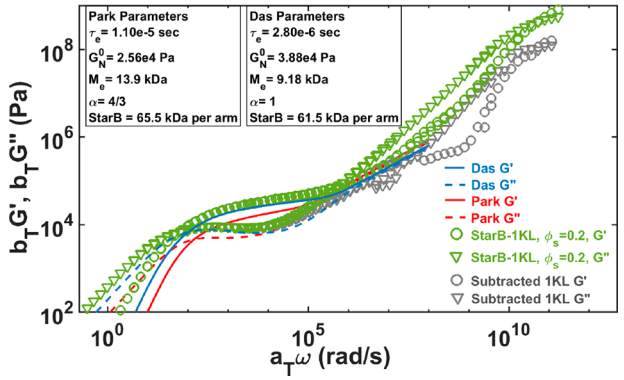

Figure 17. Same as in Figure 15, except for the 20% S−80% L blend.

1KL is removed from a given StarB−1KL blend by first horizontally shifting the 1KL relaxation moduli so that the high-frequency glassy crossover superimposes on that of the StarB−1KL blend in question. Then, the 1KL moduli are multiplied by the volume fraction of 1KL linear polymer comprising the StarB−1KL blend in question. The resulting 1KL relaxation moduli are then subtracted from the respective StarB−1KL blend data. The same procedure was used for Figure 13, discussed earlier.

In Figure 15, the rheological data after subtracting the 1KL contributions deviate from the original experimental data in the region near the onset to the glassy plateau, where the subtraction produces a factor of 2 shift in the G' and G'' moduli along the y-axis. The difference between the data with the 1KL rheology subtracted and those of the uncorrected StarB−1KL blend becomes minimal at frequencies below that of the middle crossover of G' and G'', where the Rouse modes gain dominance over the glassy modes with decreasing frequency. Upon entering the plateau region, there is no difference between the subtracted 1KL and the blend data. Also in Figure 15, the Hierarchical model with Das parameters yields predictions that are in reasonable agreement with the experimental StarB−1KL ϕ_s = 0.5 data in the terminal and plateau regions and also captures the Rouse modes of the experimental data after the influence of the 1KL is subtracted out. However, there is some discrepancy between predictions with the Das parameters and the experimental data in the plateau region. The Park parameters give no better predictions in this region and underpredict the terminal relaxation time by almost an order of magnitude. The Das and Park parameters used in Figures 15−17 are obtained from the values for the melt, given in Figure 14, by applying to these melt values the scaling formulas in eqs 1−3, with the appropriate value of α, including the adjustment for change in friction, yielding the values given in the legends in Figures 15−17.

Similarly to Figure 15, Figure 16 shows that the difference between the data with 1KL contribution subtracted and the original StarB−1KL ϕ_s = 0.4 blend data is most notable in the Rouse and glassy mode regions, with a difference slightly greater than a factor of 2 near the glassy crossover. This deviation between the two sets of curves extends over a larger frequency range than in Figure 15, which is due to the increased volume fraction of the 1KL in the ϕ_s = 0.4 blend.

For neither the Das nor Park parameters do the Hierarchical predictions in Figure 16 agree well with the experimental data. However, in the terminal regime, the Park predictions deviate from experimental terminal data by at least 1 order of magnitude along the x-axis, while for the Das parameters, the deviation is significantly less than this. The plateau modulus for both predictions is too low. Both predictions within the plateau region deviate from experimental data by roughly 30% along the y-axis. However, predictions for both Park and Das parameters are in reasonably good agreement within the Rouse region near the intermediate crossover with the data for which the 1KL contribution has been subtracted.

Because the volume fraction of linear polymer for the StarB−1KL blend series is largest for the ϕ_s = 0.2 blend, the difference between the subtracted 1KL plot and the ϕ_s = 0.2 is more notable in Figure 17 than for the blends featured in Figures 15 and 16. Near the glassy plateau, the data with 1KL rheology subtracted deviate from the original blend by at least a factor of 3 along the y-axis. In addition, the frequency range over which these two data deviate from each other is notably larger than in Figures 15 and 16. The predictions using Das parameters are in better agreement with the experimental data for which the 1KL data were subtracted both in the regime dominated by local Rouse modes and in the terminal regime. Predictions using the Park parameters, on the other hand, capture the Rouse modes but fail to capture the terminal relaxation and show a horizontal shift of almost a decade along

DOI: 10.1021/acs.macromol.8b01828
Macromolecules 2019, 52, 1757−1771

the x-axis in the terminal region. Note that these comparisons between the predictions using $\alpha = 1$ and $\alpha = 4/3$ are "fair" comparisons since the molecular weight of the star arm was adjusted for each value of α, so that equally good predictions were obtained for the pure stars, as shown in Figure 14. Given equal chances to succeed, the value $\alpha = 4/3$ fails notably when the best-fit value of molecular weight is taken for each value of α in the melt. Figures 15−17, along with Figures 9−13, strongly suggest that the Das parameters, with $\alpha = 1$, provide better predictions in the terminal regime than do the Park parameters, for which $\alpha = 4/3$. However, neither prediction is perfect because of either imperfect synthesis or characterization and/or deficiencies in the tube model used for the predictions. These deficiencies only serve to emphasize once again the importance of the use of the scaling plots in Figures 9−12, which provide a robust test of the value of α. Best fits of tube model predictions to one or a few sets of star or linear rheological data cannot overcome the uncertainties introduced by unavoidable limitations in synthesis and characterization, the parameter values, and the tube model itself.

One might argue that the proper dilution exponent to use when the dilution is gradual, or "dynamic", as envisioned in the original theory, is different from that for "static" dilution as we have explored here, where the diluting effect is due to addition of an unentangled species. A hint that this might be the case can be found in Matsumiya et al.,[64] who showed (in the Supporting Information) that there are differences in the ratio of constraint-release time to terminal time of linear polystyrene and linear polyisoprene at fixed number of entanglements Z. This implies that the three parameters $G_N^0 \tau_e$, and Z are not the only material-dependent parameters controlling relaxation of entangled polymers but that the constraint-release dynamics are governed by an additional material-dependent property. Conceivably, this nonuniversal additional parameter might affect dynamic dilution and its exponent while leaving the static dilution exponent at $\alpha = 1$. On the basis of the work of Shahid et al.[40] discussed in the Introduction, we acknowledge that the *effective* value of α as measured by the height of the modulus may increase from $\alpha = 1$ to $\alpha = 4/3$ if the entanglement densities of linear architectures are reduced by dilution to low enough values. This shift in the effective dilution exponent is attributed by Shahid et al. to relaxation mechanisms that reduce the modulus when the chains have limited numbers of entanglements and not to any deviation in the true value of α from $\alpha = 1$. Thus, in the work of Shahid et al., the shift in scaling of modulus to that corresponding to an effective value of $\alpha = 4/3$ appears at a critical number of entanglements per chain, not at a critical dilution level. Because we plot our crossover frequencies $\omega_{x,t}$ against the diluted number of entanglements per arm $M_a/(M_e\phi^{-\alpha})$, such a change in the *effective* α from unity would not cause any failure in superposition of the data but only in the dependence of $\omega_{x,t}$ on $M_a/(M_e\phi^{-\alpha})$. More research into branched polymer relaxation, and an improved tube model for star polymers, is likely needed to determine if there is a shift in the *effective* dilution exponent from $\alpha = 1$ to $\alpha = 4/3$ for star polymers at low entanglement densities, as there is for linear ones.

IV. CONCLUSION

Using well-characterized symmetric, 4-arm 1,4-polybutadiene star polymers of arm molecular weights of around 48, 61.5, and 70.1 kDa, blended with unentangled 1,4-polybutadiene linear polymer of molecular weight 1 kDa, only a dilution exponent of $\alpha = 1$, and not 4/3, correctly scales the change in terminal crossover frequency with dilution. In addition, the Hierarchical model using the Das parameter set with $\alpha = 1$ generally gives quite good agreement (i.e., terminal time within a factor of 2−3) with the experimental data for most (but not all) of the blends. The better agreement given by $\alpha = 4/3$ for some pure star and pure linear melt data throughout literature seems to have arisen because some error in the tube model is counteracted by using $\alpha = 4/3$ or perhaps becomes of errors in characterization of the molecular weight of the polymers. Such errors are neutralized by the methods employed here, which use the concentration scaling of the crossover frequency of a series of blends of three star polymers with an unentangled linear molecule to avoid dependence on a particular tube model and use of four different estimates of molecular weight for three different stars, which ensures robustness of our conclusion to synthesis and characterization errors. Further confidence is provided by including in our master plots of crossover frequency versus entanglement density data for all 1,4-polybutadiene stars available in the literature. We note that it has been known for some time that for a number of blends of short and long (both self-entangled) linear polymers the value $\alpha = 1$ is necessary to give a good fit. While it remains possible that for other mixtures of entangled polymers a dilution exponent of $\alpha = 4/3$ will provide a better model of polymer rheology, the results presented here seem to be the clearest demonstration that the value $\alpha = 1$ is most consistent with the most basic underlying assumptions of both the idea of a tube and with other entanglement paradigms, such as slip-link models.

■ ASSOCIATED CONTENT

Supporting Information

The Supporting Information is available free of charge on the ACS Publications website at DOI: 10.1021/acs.macromol.8b01828.

Details concerning the synthesis of StarA, StarB, and StarC; rheology and analysis of StarA−1KL, StarB−1KL and StarC−1KL blends (PDF)

■ AUTHOR INFORMATION

Corresponding Authors

*E-mail rlarson@umich.edu.
*E-mail Nikolaos.Hadjichristidis@kaust.edu.sa.

ORCID

Ryan Hall: 0000-0002-5567-4016
Sanghoon Lee: 0000-0002-8367-1787
Taihyun Chang: 0000-0003-2623-1803
Nikos Hadjichristidis: 0000-0003-1442-1714
Ronald G. Larson: 0000-0001-7465-1963

Present Addresses

¶(B.-G.K.) LG Chem, Ltd., LG Science Park, Seoul 07796, Republic of Korea.
□(D.C.V.) Department of Chemical and Materials Engineering, New Jersey Institute of Technology, Newark, New Jersey 07102, United States.

Notes

The authors declare no competing financial interest.

DOI: 10.1021/acs.macromol.8b01828
Macromolecules 2019, 52, 1757−1771

■ ACKNOWLEDGMENTS

R.H. and R.G.L. gratefully acknowledge the support of the National Science Foundation under Grants DMR 1403335 and 1707640. Any opinions, findings, and conclusions or recommendations expressed in this material are those of the authors and do not necessarily reflect the views of the National Science Foundation (NSF). N.H. gratefully acknowledges the support of the King Abdullah University of Science and Technology (KAUST).

■ REFERENCES

(1) Doi, M.; Edwards, S. F. Dynamics of Concentrated Polymer Systems Part 1: Brownian Motion in the Equilibrium State. *J. Chem. Soc., Faraday Trans. 2* **1978**, *74*, 1789−1801.
(2) Doi, M.; Edwards, S. F. Dynamics of Concentrated Polymer Systems Part 2: Molecular Motion Under Flow. *J. Chem. Soc., Faraday Trans. 2* **1978**, *74*, 1802−1817.
(3) Doi, M.; Edwards, S. F. Dynamics of Concentrated Polymer Systems Part 3: The Constitutive Equation. *J. Chem. Soc., Faraday Trans. 2* **1978**, *74*, 1818−1832.
(4) Doi, M.; Edwards, S. F. Dynamics of Concentrated Polymer Systems Part 4: Rheological Properties. *J. Chem. Soc., Faraday Trans. 2* **1979**, *75*, 38−54.
(5) de Gennes, P. G. Reptation of a Polymer Chain in the Presence of Fixed Obstacles. *J. Chem. Phys.* **1971**, *55*, 572.
(6) Tuminello, W. H. Molecular Weight and Molecular Weight Distribution from Dynamic Measurements of Polymer Melts. *Polym. Eng. Sci.* **1986**, *26*, 1339−1347.
(7) Tsenoglou, C. Viscoelasticity of Binary Homopolymer Blends. *ACS Polym. Prepr.* **1987**, *8*, 185−186.
(8) des Cloizeaux, J. Double Reptation vs. Simple Reptation in Polymer Melts. *Europhys. Lett.* **1988**, *5*, 437−442.
(9) Klein, J. The Onset of Entangled Behavior in Semidilute and Concentrated Polymer Solutions. *Macromolecules* **1978**, *11* (5), 852−858.
(10) Viovy, J.; Rubinstein, M.; Colby, R. Constraint Release in Polymer Melts: Tube Reorganization versus Tube Dilation. *Macromolecules* **1991**, *24*, 3587−3596.
(11) Daoud, M.; de Gennes, P. G. Some Remarks on the Dynamics of Polymer Melts. *J. Polym. Sci., Polym. Phys. Ed.* **1979**, *17*, 1971−1981.
(12) de Gennes, P. G. Scaling Theory of Polymer Absorption. *J. Phys. (Paris)* **1976**, *37* (12), 1445−1452.
(13) de Gennes, P. G. Dynamics of Entangled Polymer Solutions. II. Inclusion of Hydrodynamic Interactions. *Macromolecules* **1976**, *9* (4), 594−598.
(14) O'Connor, N. P. T.; Ball, R. C. Confirmation of the Doi-Edwards Model. *Macromolecules* **1992**, *25*, 5677−5682.
(15) Rubinstein, M. Discretized Model of Entangled-Polymer Dynamics. *Phys. Rev. Lett.* **1987**, *59* (17), 1946−1949.
(16) Marrucci, G. Relaxation by Reptation and Tube Enlargement: A Model for Polydisperse Polymers. *J. Polym. Sci., Polym. Phys. Ed.* **1985**, *23*, 159−177.
(17) Ball, R. C.; McLeish, T. C. B. Dynamic Dilution and the Viscosity of Star-Polymer Melts. *Macromolecules* **1989**, *22*, 1911−1913.
(18) Milner, S. T.; McLeish, T. C. B.; Young, R. N.; Hakiki, A.; Johnson, J. M. Dynamic Dilution, Constraint-Release, and Star-Linear Blends. *Macromolecules* **1998**, *31*, 9345−9353.
(19) Larson, R. G. Combinatorial Rheology of Branched Polymer Melts. *Macromolecules* **2001**, *34*, 4556−4571.
(20) Park, S. J.; Shanbhag, S.; Larson, R. G. A Hierarchical Algorithm for Predicting the Linear Viscoelastic Properties of Polymer Melts with Long-Chain Branching. *Rheol. Acta* **2005**, *44*, 319−330.
(21) Wang, Z.; Chen, X.; Larson, R. G. Comparing Tube Models for Predicting the Linear Rheology of Branched Polymer Melts. *J. Rheol.* **2010**, *54*, 223−260.
(22) Das, C.; Inkson, N. J.; Read, D. J.; Kelmanson, M. A.; McLeish, T. C. B. Computational Linear Rheology of General Branch-on-Branch Polymers. *J. Rheol.* **2006**, *50* (2), 207−234.
(23) Ebrahimi, T.; Taghipour, H.; Grießl, D.; Mehrkhodavandi, P.; Hatzikiriakos, S. G.; van Ruymbeke, E. Binary Blends of Entangled Star and Linear Poly(hydroxybutyrate): Effect of Constraint Release and Dynamic Tube Dilation. *Macromolecules* **2017**, *50*, 2535−2546.
(24) Doi, M.; Graessley, W. W.; Helfand, E.; Pearson, D. S. Dynamics of Polymers in Polydisperse Melts. *Macromolecules* **1987**, *20*, 1900−1906.
(25) Watanabe, H.; Ishida, S.; Matsumiya, Y.; Inoue, T. Viscoelastic and Dielectric Behavior of Entangled Blends of Linear Polyisoprenes having Widely Separated Molecular Weights. *Macromolecules* **2004**, *37*, 1937−1951.
(26) Watanabe, H.; Ishida, S.; Matsumiya, Y.; Inoue, T. Test of Full and Partial Tube Dilation Pictures in Entangled Blends of Linear Polyisoprenes. *Macromolecules* **2004**, *37*, 6619−6631.
(27) Huang, Q.; Hengeller, L.; Alvarez, N. J.; Hassager, O. Bridging the Gap between Polymer Melts and Solutions in Extensional Rheology. *Macromolecules* **2015**, *48*, 4158−4163.
(28) Milner, S. T. Predicting the Tube Diameter in Melts and Solutions. *Macromolecules* **2005**, *38*, 4929−4939.
(29) Colby, R. H.; Rubinstein, M. Two-Parameter Scaling for Polymers in Θ Solvents. *Macromolecules* **1990**, *23*, 2753−2757.
(30) Park, S. J.; Larson, R. G. Modeling the Linear Viscoelastic Properties of Metallocene-Catalyzed High Density Polyethylenes with Long-Chain Branching. *J. Rheol.* **2005**, *49*, 523−536.
(31) Park, S. J.; Larson, R. G. Tube Dilation and Reptation in Binary Blends of Monodisperse Linear Polymers. *Macromolecules* **2004**, *37*, 597−604.
(32) Park, S. J.; Larson, R. G. Dilution Exponent in the Dynamic Dilution Theory for Polymer Melts. *J. Rheol.* **2003**, *47*, 199−211.
(33) Milner, S. T.; McLeish, T. C. B. Parameter-Free Theory for Stress Relaxation in Star Polymer Melts. *Macromolecules* **1997**, *30*, 2159−2166.
(34) Daniels, D. R.; McLeish, T. C. B.; Kant, R.; Crosby, B. J.; Young, R. N.; Pryke, A.; Allgaier, J.; Groves, D. J.; Hawkins, R. J. Linear Rheology of Diluted Linear, Star and Model Long Chain Branched Polymer Melts. *Rheol. Acta* **2001**, *40*, 403−415.
(35) Raju, V. R.; Menezes, E. V.; Marin, G.; Graessley, W. W.; Fetters, L. J. Concentration and Molecular Weight Dependence of Viscoelastic Properties in Linear and Star Polymers. *Macromolecules* **1981**, *14*, 1668−1676.
(36) Tao, H.; Huang, C.; Lodge, T. P. Correlation Length and Entanglement Spacing in Concentrated Hydrogenated Polybutadiene Solutions. *Macromolecules* **1999**, *32*, 1212−1217.
(37) Brochard, F.; de Gennes, P. G. Dynamical Scaling for Polymers in Theta Solvents. *Macromolecules* **1977**, *10* (5), 1157−1161.
(38) van Ruymbeke, E.; Masubuchi, Y.; Watanabe, H. Effective Value of the Dynamic Dilution Exponent in Bidisperse Linear Polymers: From 1 to 4/3. *Macromolecules* **2012**, *45*, 2085−2098.
(39) van Ruymbeke, E.; Shchetnikava, V.; Matsumiya, Y.; Watanabe, H. Dynamic Dilution Effect in Binary Blends of Linear Polymers with Well-Separated Molecular Weights. *Macromolecules* **2014**, *47*, 7653−7665.
(40) Shahid, T.; Huang, Q.; Oosterlinck, F.; Clasen, C.; van Ruymbeke, E. Dynamic Dilution Exponent in Monodisperse Entangled Polymer Solutions. *Soft Matter* **2017**, *13*, 269−282.
(41) Desai, P. S.; Kang, B.; Katzarova, M.; Hall, R.; Huang, Q.; Lee, S.; Shivokhin, M.; Chang, T.; Venerus, D. C.; Mays, J.; Schieber, J. D.; Larson, R. G. Challenging Tube and Slip-Link Models: predicting the Linear Rheology of Blends of Well-Characterized Star and Linear 1,4-Polybutadienes. *Macromolecules* **2016**, *49* (13), 4964−4977.
(42) Andreev, M.; Khaliullin, R. N.; Steenbakkers, R. J.; Schieber, J. D. Approximations of the Discrete Slip-Link Model and their Effect on Nonlinear Rheology Predictions. *J. Rheol.* **2013**, *57*, 535−557.
(43) Schieber, J. D. Fluctuations in Entanglements of Polymer Liquids. *J. Chem. Phys.* **2003**, *118*, 5162−5166.

DOI: 10.1021/acs.macromol.8b01828
Macromolecules 2019, 52, 1757−1771

(44) Khaliullin, R. N.; Schieber, J. D. Self-Consistent Modeling of Constraint Release in a Single-Chain Mean-Field Slip-Link Model. *Macromolecules* **2009**, *42* (19), 7504−7517.
(45) Neergaard, J.; Schieber, J. D. A Full-Chain Network Model with Sliplinks and Binary Constraint Release. *Proc. XIIIth Int. Cong. Rheol.* **2000**.
(46) Schieber, J. D.; Neergaard, J.; Gupta, S. A Full-Chain, Temporary Network Model with Sliplinks, Chain-Length Fluctuations, Chain Connectivity and Chain Stretching. *J. Rheol.* **2003**, *47*, 213−233.
(47) Schieber, J. D. GENERIC Compliance of a Temporary Network Model with Sliplinks, Chain-Length Fluctuations, Segment-Connectivity and Constraint Release. *J. Non-Equilib. Thermodyn.* **2003**, *28*, 179−188.
(48) Heo, Y.; Larson, R. G. The Scaling of Zero-Shear Viscosities of Semidilute Polymer Solutions with Concentration. *J. Rheol.* **2005**, *49*, 1117−1128.
(49) Lipson, J. E. G.; Milner, S. T. Multiple Glass Transitions and Local Composition Effects on Polymer Solvent Mixtures. *J. Polym. Sci., Part B: Polym. Phys.* **2006**, *44*, 3528−3545.
(50) McLeish, T. Tube Theory of entangled Polymer Dynamics. *Adv. Phys.* **2002**, *51* (6), 1379−1527.
(51) Larson, R. G.; Sridhar, T.; Leal, L. G.; McKinley, G. H.; Likhtman, A. E.; McLeish, T. C. B. Definitions of Entanglement Spacing and Time Constants in the Tube Model. *J. Rheol.* **2003**, *47*, 809−818.
(52) Hadjichristidis, N.; Iatrou, H.; Pispas, S.; Pitsikalis, M. Anionic Polymerization: High Vacuum Techniques. *J. Polym. Sci., Part A: Polym. Chem.* **2000**, *38*, 3211.
(53) Hadjichristidis, N.; Roovers, J. Linear Viscoelastic Properties of Mixtures of 3- and 4-arm Polybutadiene Stars. *Polymer* **1985**, *26*, 1087.
(54) Polymeropoulos, G.; Zapsas, G.; Ntetsikas, K.; Bilalis, P.; Gnanou, Y.; Hadjichristidis, N. 50th Anniversary perspective: Polymers with Complex Architectures. *Macromolecules* **2017**, *50*, 1253.
(55) Park, S. J.; Desai, P. S.; Chen, X.; Larson, R. G. Universal Relaxation Behavior of Entangled 1,4-Polybutadiene Melts in the Transition Frequency Region. *Macromolecules* **2015**, *48*, 4122−4131.
(56) Palade, L. I.; Verney, V.; Attané, P. Time-Temperature Superposition and Linear Viscoelasticity of Polybutadienes. *Macromolecules* **1995**, *28*, 7051−7057.
(57) Colby, R. H.; Fetters, L. J.; Graessley, W. W. The Melt Viscosity-Molecular Weight Relationship for Linear Polymers. *Macromolecules* **1987**, *20* (9), 2226−2237.
(58) Li, S. W.; Park, H. E.; Dealy, J. M. Evaluation of Molecular Linear Viscoelastic Models for Polydisperse H Polybutadienes. *J. Rheol.* **2011**, *55* (6), 1341−1373.
(59) Shivokhin, M. E.; van Ruymbeke, E.; Bailly, C.; Kouloumasis, D.; Hadjichristidis, N.; Likhtman, A. E. Understanding Constraint Release in Star/Linear Polymer Blends. *Macromolecules* **2014**, *47* (7), 2451−2463.
(60) Miros, A.; Vlassopoulos, D.; Likhtman, A. E.; Roovers, J. Linear Rheology of Multiarm Star Polymers Diluted with Short Linear Chains. *J. Rheol.* **2003**, *47* (1), 163−176.
(61) Wagner, M. H. Scaling Relations for Elongational Flow of Polystyrene Melts and Concentrated Solutions of Polystyrene in Oligomeric Styrene. *Rheol. Acta* **2014**, *53*, 765−777.
(62) Roovers, J. Properties of the Plateau Zone of Star-branched Polybutadienes and Polystyrenes. *Polymer* **1985**, *26*, 1091−1095.
(63) Rochefort, W. E.; Smith, G. G.; Rachapudy, H.; Raju, V. R.; Graessley, W. W. Properties of Amorphous and Crystallizable Hydrocarbon Polymers. II. Rheology of Linear and Star-Branched Polybutadiene. *J. Polym. Sci., Polym. Phys. Ed.* **1979**, *17*, 1197−1210.
(64) Struglinski, M. J.; Graessley, W. W.; Fetters, L. J. Effects of Polydispersity on the Linear Viscoelastic Properties of Entangled Polymers. 3. Experimental Observations on Binary Mixtures of Linear and Star Polybutadienes. *Macromolecules* **1988**, *21*, 783−789.
(65) Matsumiya, Y.; Kumazawa, K.; Nagao, M.; Urakawa, O.; Watanabe, H. Dielectric relaxation of Monodisperse Linear Polyisoprene: Contribution of Constraint Release. *Macromolecules* **2013**, *46*, 6067−6080.

DOI: 10.1021/acs.macromol.8b01828
Macromolecules 2019, 52, 1757−1771